



NeuroCamTags: Long-Range, Battery-free, Wireless Sensing with Neuromorphic Cameras

DANNY SCOTT, University of Tennessee Knoxville, USA

MATTHEW BRINGLE, University of Tennessee Knoxville, USA

IMRAN FAHAD, University of Tennessee Knoxville, USA

GADDIEL MORALES, University of Tennessee Knoxville, USA

AZIZUL ZAHID, University of Tennessee Knoxville, USA

SAI SWAMINATHAN, University of Tennessee Knoxville, USA

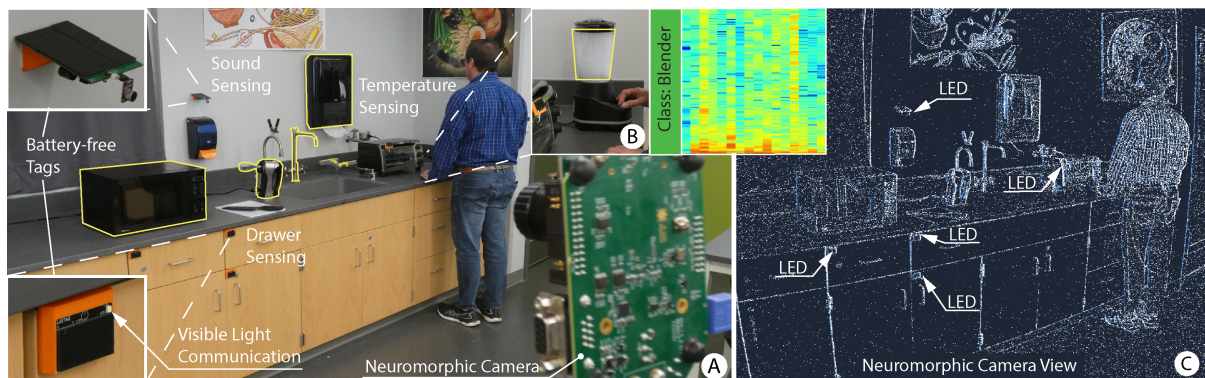


Fig. 1. Battery-free wireless tags **A.** NeuroCamTags in a smart kitchen environment, monitoring object activity (highlighted in yellow: microwave, mixer, faucet, paper towel, blender), toaster oven temperature, and drawer activity. **B.** Spectrogram of microphone modulated LED signal and machine learning activity classification as a blender. **C.** Neuromorphic camera view of smart kitchen environment from a 2000 microseconds (μ s) timeframe moment.

In this research, we introduce NeuroCamTags, a battery-free platform designed to detect a range of rich human interactions and activities in entire rooms and floors without the need for batteries. The NeuroCamTag system comprises low-cost tags that harvest ambient light energy and utilize high-frequency modulation of light-emitting diodes (LEDs) for wireless communication. These visual signals are captured by an available neuromorphic camera, which boasts temporal resolution and frame rates an order of magnitude higher than those of conventional cameras. We present an event processing pipeline that allows simultaneous localization and identification of multiple unique tags. NeuroCamTags offer a wide range of functionalities, providing battery-free wireless sensing for various physical stimuli, including changes in temperature, contact, button presses, key presses, and even sound cues. Our empirical evaluations demonstrate impressive accuracy at long ranges up to 200

Authors' Contact Information: [Danny Scott](mailto:dscott57@vols.utk.edu), dscott57@vols.utk.edu, University of Tennessee Knoxville, Tennessee, USA; [Matthew Bringle](mailto:matthewbringle@utk.edu), University of Tennessee Knoxville, USA; [Imran Fahad](mailto:imran.fahad@utk.edu), University of Tennessee Knoxville, USA; [Gaddiel Morales](mailto:gaddiel.morales@utk.edu), University of Tennessee Knoxville, USA; [Azizul Zahid](mailto:azizul.zahid@utk.edu), University of Tennessee Knoxville, USA; [Sai Swaminathan](mailto:sai.swaminathan@utk.edu), University of Tennessee Knoxville, USA.

Permission to make digital or hard copies of all or part of this work for personal or classroom use is granted without fee provided that copies are not made or distributed for profit or commercial advantage and that copies bear this notice and the full citation on the first page. Copyrights for components of this work owned by others than the author(s) must be honored. Abstracting with credit is permitted. To copy otherwise, or republish, to post on servers or to redistribute to lists, requires prior specific permission and/or a fee. Request permissions from permissions@acm.org.

© 2024 Copyright held by the owner/author(s). Publication rights licensed to ACM.

ACM 2474-9567/2024/9-ART122

<https://doi.org/10.1145/3678529>

feet. In addition to these findings, we consider a range of applications such as battery-free input devices, tracking of human movement, and long-range detection of human activities in various environments such as kitchens, workshops, etc. By reducing reliance on batteries, NeuroCamTags promotes eco-friendliness and opens doors to exciting possibilities in smart environment technology.

CCS Concepts: • Human-centered computing → Ubiquitous and mobile computing systems and tools; Interaction devices.

Additional Key Words and Phrases: Activity sensing; Battery-free; Wireless sensing; Context Aware Computing;

ACM Reference Format:

Danny Scott, Matthew Bringle, Imran Fahad, Gaddiel Morales, Azizul Zahid, and Sai Swaminathan. 2024. NeuroCamTags: Long-Range, Battery-free, Wireless Sensing with Neuromorphic Cameras. *Proc. ACM Interact. Mob. Wearable Ubiquitous Technol.* 8, 3, Article 122 (September 2024), 25 pages. <https://doi.org/10.1145/3678529>

1 Introduction

For decades, smart environments have promised to improve our lives by inferring context, actions, and activities in various settings, from public areas and offices to homes, workshops, factories, and healthcare centers. To achieve this vision, one of the most commonly adopted methods for making dumb environments “smart” is using embedded cameras. However, only using cameras is limited by the richness of the data that they capture. For instance, most camera approaches capture just visual information, and therefore, they are fused with data from different sensing modalities to capture human touch, temperature, audio, pressure, etc. However, using these smart devices (both cameras and sensors) for perpetual sensing of human environments has not yet been realized due to two major issues: power and privacy. Smart devices such as cameras and sensors are defined by short battery lifetimes, high maintenance costs, and rapid obsolescence, contributing to the explosion of electronic waste in the past decades [10, 18]. Replacement of billions of batteries (per year) that power these sensors would be unsustainable and have high costs. The ecological impacts of computing with batteries have become clearer and clearer [16].

Fortunately, emerging paradigms for cameras, such as neuromorphic cameras [13, 35], present numerous benefits, including low-power operation, extremely rapid response times down to microseconds (μ s), and enhanced privacy due to their reduced data capture compared to standard cameras (see Figure 1 C). In our research, we introduce *NeuroCamTags*—a hardware platform for building a collection of battery-free interactive devices that harness the unique capabilities of neuromorphic cameras to foster eco-friendly intelligent spaces. We designed NeuroCamTags as solar-powered devices capable of sensing user interactions and wirelessly transmitting data via high-frequency LED modulation. We then detect these light signals over considerable distances using neuromorphic cameras due to their superior high dynamic range (HDR) and rapid temporal resolution compared to the frame rates and HDR capabilities of traditional cameras. For example, we show a range of battery-free wireless sensors and interactive devices in Figures 1 and 2. NeuroCamTag sensors are capable of monitoring object use, environment variables, and user interaction. In Figure 2, we see the temperature of the glue gun held by a user in the workshop as far away as 70 feet from the camera in our 160 feet by 100 feet maker space environment.

In this paper, we describe the design and implementation of NeuroCamTags: circuit designs, sensors, energy harvesting, and energy management methods. We investigated modulation methods for embedding sensor data, including On-Off Keying (OOK) and frequency modulation (FM), optimized for optical wireless communication with neuromorphic cameras. We further discuss the software pipeline developed for demodulation, signal processing, and the application of machine learning to interpret the data acquired by neuromorphic cameras for the detection of NeuroCamTags and the analysis of user activity. We present our experimental findings on the operational efficiency of NeuroCamTags in various scenarios—covering diverse distances, lighting conditions,

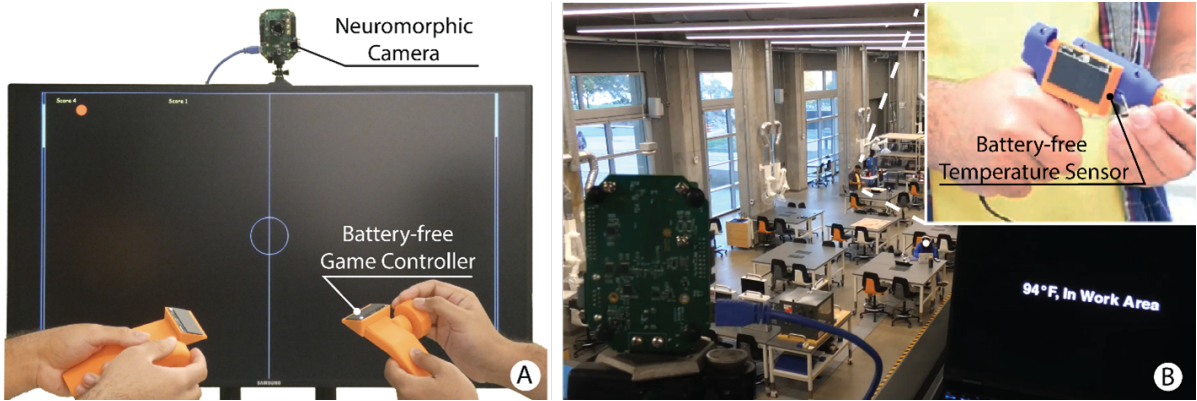


Fig. 2. Human interaction and sensing **A.** Playing an interactive game of pong with multiple battery-free game controllers. **B.** Sending temperature sensor reading and localization information wirelessly over a long range (70 feet)

and angles of view, as well as their application in assorted intelligent settings such as workshops and kitchens. Our system can recognize user interactions with an accuracy of 96.3% and maintains a false positive rate of 3.4%. Our studies also reveal the capability of our tags to function effectively from distances up to 200 feet. Furthermore, we examine the specifics of power usage of our devices, noting the minimal light levels (500 lux) required for battery-free operation and the data transmission rates needed for functionality. We conclude by showcasing 11 practical applications we developed, demonstrating the broad capabilities and potential uses of NeuroCamTags.

Overall, we believe this work introduces a new sensing approach for smart environments with unique strengths to contribute to human-computer interaction (HCI) researchers. We make the following contributions to this work:

- An end-to-end system including hardware, and signal processing algorithms, for battery-free smart environment sensing based on neuromorphic cameras.
- Custom circuits that integrate sensing, energy harvesting, voltage regulation, and embedded computation. These circuits are uniquely designed for both analog and digital visible light communication (VLC) with neuromorphic cameras, optimizing power consumption and operational range.
- Empirical Evaluation of the usable range, distance, power and transmission speed of NeuroCamTags under various conditions
- A proof-of-concept demonstration and technical validation of activity detection in two smart environments instrumented with NeuroCamTag wireless sensors.

2 Background and Related Work

Neuromorphic vision sensors are inspired by the design of the human eye's rods and cones in detecting light. Similar to the human eye, image signals are processed individually across pixels in these sensors. Unlike standard RGB cameras that capture entire scenes, neuromorphic cameras monitor changes in brightness (polarity) for each pixel, doing so with remarkable speed and minimal delay. They offer six key benefits for vision-based sensing compared to traditional cameras:

Pixel-level Independence: Each pixel in a neuromorphic camera operates independently and asynchronously (see Figure 1 C). Instead of capturing frames at a fixed rate, each pixel in the sensor detects changes in intensity independently and only responds when it sees a change.

Low Latency: Since pixels respond to changes immediately, the latency can be extremely low, often in the order of microseconds, significantly faster than the milliseconds typical of conventional cameras.

High Dynamic Range (HDR): Event cameras are known for their high dynamic range, often exceeding 120 dB compared to about 60-70 dB for standard cameras. This enables them to work well in both very bright and very dark environments without the typical over or underexposure problems.

Power Efficiency: By only sending information when changes are detected, event cameras typically consume substantially less power [12], making them efficient for edge IoT applications.

Reduced Data: As they only output data when changes in the scene occur, event cameras can generate far less data than traditional cameras, which capture the entire scene at regular intervals. This can reduce storage and processing requirements.

Temporal Resolution: The asynchronous nature of the pixel response allows for very high temporal resolution, capturing quick changes in a scene that might be missed by the slower frame rates of traditional cameras.

These advantages underscore the potential of neuromorphic cameras for energy efficient sensing and visible light communication. An array of recent related has explored the use of neuromorphic camera for diverse applications. For instance, work by Kueng et al. [22], Craig et al. [19], and Zhou et al. [64] has showcased event cameras in visual odometry and tracking mobile ground robots. In the realm of driver monitoring systems, Shariff et al. [46] have demonstrated the effectiveness of event cameras even under dynamically changing scene lighting. Mueggler et al. [29] achieved 6-DOF pose tracking for high-speed maneuvers using event-based methods.

The field of non-contact signal acquisition and fault diagnosis has also advanced significantly, with Guang et al. [17] introducing a method for integrating machine-generated event data into precise vibration signal extraction and fault diagnosis. In emergency detection and alerting systems, Costa et al. [8] developed systems for urban, agricultural, and industrial settings using neuromorphic cameras.

Pertinent to our work, Chen et al. [7] created a system for accurately identifying high-frequency flickering LEDs in indoor positioning using neuromorphic cameras. Wang et al. [54] developed a beacon system with flickering high-frequency LEDs for robotic communication. In the field of human-computer interaction, neuromorphic cameras have been used for gesture detection [2] and, more recently, for activity recognition from an egocentric perspective [34]. For an in-depth understanding of neuromorphic cameras, we recommend the work by Gallego et al. [14], which discusses camera principles, sensors, applications, challenges, and future directions in machine perception.

To the best of our knowledge, our work is one of the first to employ neuromorphic cameras for battery-free sensing and visible light wireless communication of human interactions within smart environments. This includes integrating multiple modalities such as temperature, audio, touch, and various input devices.

3 Design Considerations

There are several key design requirements we sought to achieve with NeuroCamTag system.

- **D1. Self-powered, battery-and maintenance-free operation:** In a smart environment where sensing devices need to be pervasively deployed, the tags must operate for long periods without maintenance. The tags should be self-powered via energy harvesting and operate without batteries.
- **D2. Support rich wireless input:** The sensing devices should go beyond presence detection and user input. The tags should support a rich array of wireless interactions to include continuous input events, touch, temperature, pressure, voice based control, detect audio events or even multi-modal interactions to fit the environment and user needs.
- **D3. Support for adaptability and no device programming:** Lighting conditions in the built environment vary widely; therefore, the design of tags should support different lighting conditions by allowing modular

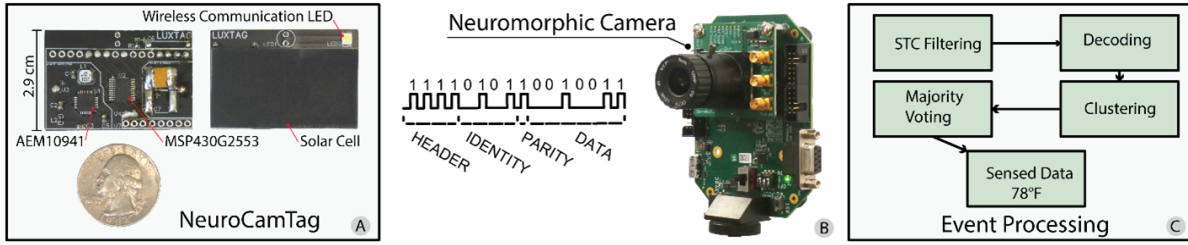


Fig. 3. Digital NeuroCamTag System Overview **A.** Battery-free wireless NeuroCamTag back and front view. **B.** Neuromorphic camera receiving OOK modulated light signal from NeuroCamTag. **C.** Flow chart of the event processing pipeline decoding OOK message from sensor.

energy harvesting. Besides lighting, some tags should require no hardware programming, i.e., tags that operate by simple hardware components.

- **D4. Minimize components and cost:** The cost per sensing device (each NeuroCamTag) should be under \$10-\$20 to achieve meaningful deployment as environments outfitted with 100s of sensors are scalable at lower price points. To achieve lower costs, a single tag should have less than 15 components.

Taking into account these design goals, two tags were designed – *Digital NeuroCamTag* and *Analog NeuroCamTag*. These tags embody many of the design goals discussed above such as designing, developing, and validating our approach for interactive wireless sensors with neuromorphic cameras. While both analog and digital NeuroCamTags are self-powered (D1), support rich input sensing (D2), and wirelessly communicate with the camera at long distances using light from LEDs, there are some key differences. For instance, the digital NeuroCamTag uses an OOK modulation scheme and is much more power efficient and able to operate in a low lux environment (even 500 lux), as power is not needed for communicating a logic "0". On the other hand, our analog NeuroCamTag is "always on" and uses frequency modulation (FM) to communicate with the camera. In addition to power, the sensing and wireless communication in the analog NeuroCamTag is achieved by using a voltage-controlled oscillator (555 timer). The 555 timer is "capacitor/resistor programmable", requiring no software programming (D3) and are adaptable to varying light levels, as modular solar panels can be added or removed. Finally, both our tags consist of less than 15 components, lowering deployment costs (D4).

As outlined in our background section, neuromorphic cameras function asynchronously at the pixel level, enabling us to detect signals from multiple tags simultaneously during interactive events. Specifically, we use the EVK3HD neuromorphic camera, featuring 1 Mega Pixel from Prophesee [36], to process the visual signals emitted by our tags. While the camera we use is an evaluation kit camera, more recently, neuromorphic cameras that operate with STM32 microcontroller units (MCUs) are available for mass adoption [37].

4 Digital NeuroCamTag System Overview

In this section, we present a comprehensive overview of the digital NeuroCamTag System, as depicted in Figure 3. The system consists of two primary elements: the tag hardware and a software pipeline for processing input sensor data and detecting digital tags. These tags utilize ambient light for power; they detect user interaction, sense the environment, and transmit digital data wirelessly via light signals. The neuromorphic camera, positioned in a secluded, out-of-the-way area with a clear view of the tags, such as on the wall or up in the corner of a room, is able to constantly monitor the tag's activity. Upon receiving messages, our software algorithm first applies a filtering process that removes non-messages by the identified header. Following this, the decoding algorithm takes over, clustering messages from various digital tags to accurately extract and interpret the sensor data.

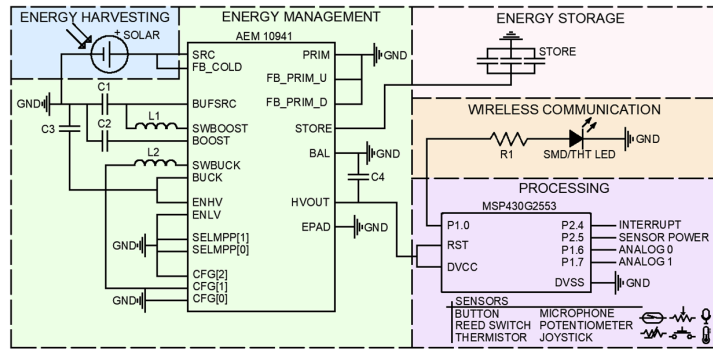


Fig. 4. Digital NeuroCamTag schematic

4.1 Hardware Design

Our digital NeuroCamTag hardware is broken down into energy harvesting, energy management, storage, sensing, computing with ultra-low-power MCU, and wireless communication. Figure 4 shows the layout of the circuit modules and the components chosen to optimize for self-powered operation.

Energy Harvesting: We utilize the IXOLAR SM141K06L solar panel to harvest ambient solar energy. This panel has dimensions of 1.654 inches X 0.906 inches X 0.083 inches and has a weight of 3.4 grams. It is designed to deliver an open-circuit voltage of 4.15 volts, though actual performance can fluctuate depending on the intensity of available light.

During our development phase, we evaluated a range of smaller solar panels, including models SM730K12L and KXOB25-05X3F, which differed in both size and photocurrent generation. Interactive user input necessitates both high-speed responsiveness due to constant sensing and continuous wireless communications capable of handling several messages per second, for example, for playing games like pong, using a battery-free wireless controller with knobs. The chosen solar panel meets our power requirements most effectively, offering an optimal balance of size, weight, power, and cost (SWAP-C) in relation to the predetermined message length (see §6.6).

Energy Management and Storage: The power output of solar panels fluctuates due to the varying lighting conditions (e.g. changing sunlight) of the environment, as well as user interaction, such as moving a battery-free input device. To provide stable voltage, we investigated several buck-boost devices such as LTC3808, BQ25570, etc., and finally chose AEM10941 due to its ultra-low cold start voltage of 380mV, startup current of 7.8 μ A and a quiescent current draw of <1 μ A(Iq). Finally, in addition to harvesting, we support capacitor based energy storage for battery-free operation. Our circuits support capacitor banks that can be soldered. We chose tantalum capacitors (ranging from 680 μ F to 0.4F) as they offer the lowest DC leakage properties and lowest equivalent series resistance (ESR). The choice of capacitor used depends on the bootup time vs storage capacity desired. In section §6.6, we detail trade-offs for choosing capacitor values.

MCU and Computation: When a sufficient voltage (3.3v) is achieved by energy harvesting, the AEM10941 chip onboard delivers power to our ultra-low-power 16-bit MCU MSP430G2553 that operates in five low power modes (LPM4, LPM3, LPM2, LPM1, LPM0). The lowest mode (LPM4) consumes as little as 80 μ A. We selected the MSP430 microcontroller due to its lower power operation, ease of use, the availability of open-source firmware libraries and toolchains, and its established presence within the embedded systems community. Our MCU switches between the different LPM modes between input sensing and wireless communication. For example, pressing a button triggers an interrupt from LPM4 (deep sleep), waking up the MCU into its active state for wireless communication and returning back to deep sleep mode (LPM4) to save power. Although LPM4 is the lowest, not

all interactions can operate in that mode due to the clock requirement for an ADC read. Therefore, only button press interactions switch between LPM4, whereas other interactions using ADC read, such as a temperature, moving a slider, rotating a knob, etc., operate between LPM3 and the active state.

Encoding Input Data and Wireless Communication: Our MCU employs a digital On-Off-keying (OOK) to transmit interactive events and sensor data by modulating LEDs wirelessly. We chose OOK for its power-saving advantage—when transmitting the binary sequence of "1" and "0", the LED remains on for '1' and off for the representation of '0', conserving power. Specifically, we calculate the LED's "on" time for a binary '1' by using formula 1 below:

$$\text{Half Bit On/Off Time} = \left(\frac{1}{BPS} \times \frac{1}{2} \right) \text{ms} \quad (1)$$

leading to significant energy savings, as no power is consumed during the '0' intervals. For instance, with a transmission rate of 1000 Bits Per Second (BPS), the LED lights up for just 500 microseconds for each '1' bit. As depicted in Figure 3, each digital NeuroCamTag message is comprised of 16 bits divided into four distinct segments: a 4-bit header for synchronization, a 4-bit identifier for tagging up to 16 unique tags, a single-bit parity for error reduction, and a 7-bit payload for data representation. The 7-bit payload was selected to accommodate a sufficient range of analog inputs (0-127), such as those from dials, sliders, or temperature sensors. For example, a temperature reading of 76° would be transmitted as its 7-bit binary counterpart (1001100). The 4-bit header is optimized for message synchronization with our camera's decoding algorithm (detailed in §4.1)

4.2 Software Pipeline

We now discuss our camera software for decoding wireless transmission from digital NeuroCamTags. Neuromorphic cameras capture encoded light signals as they can operate with high temporal resolution and detect changes within 100s of microseconds.

Filtering: Before we begin processing our signal, we employ the camera's spatial-temporal contrast filter (STC) to reduce noise. The STC filter works by analyzing camera input contrast across a scene over time and removes isolated events. This filter is particularly useful in scenarios where both the spatial relationships between objects and their changes over time are important.

Decoding: After filtering, when the first encoded message bit arrives, the decoding process starts. For instance, when a "1" bit arrives, which corresponds to an LED turned on, an event is logged as $e_1(p_1, t_1, x_1, y_1)$, where p_1 is the polarity of the event, t_1 is the timestamp, x_1, y_1 are the coordinates. Following the first event, when the LED turns off at timestamp t_2 , it generates a second event with a polarity of 0 at the same coordinate (see Figure 5).

- For each XY coordinate our algorithm creates a double-ended queue. As events arrive, they are continuously added to the appropriate double-ended queue by each coordinate. The events are also checked to ensure they do not exceed the expected message time threshold (Th_1). An event occurring after the threshold prompts the processing of all queues up to Th_1 at various coordinates, as shown in Figure 5C.
- While processing these queues during the second step, our camera software inserts "0's" in queues where significant time lapses follow a polarity shift from 0 to 1 or 1 to 0, as depicted in Figure 5 with long gray blocks.
- As a third step, the software converts queues into message candidates. During this step the parity bit is verified. Message candidates with incorrect parity are discarded.
- As the fourth and final step, the software gathers message candidates from various coordinates. These messages undergo a k-means clustering process as well as a majority voting process, where the most common message is selected as the output. The k-means algorithm is chosen for its computational efficiency, with the 'k' value determined by the number of tags present in the scene.

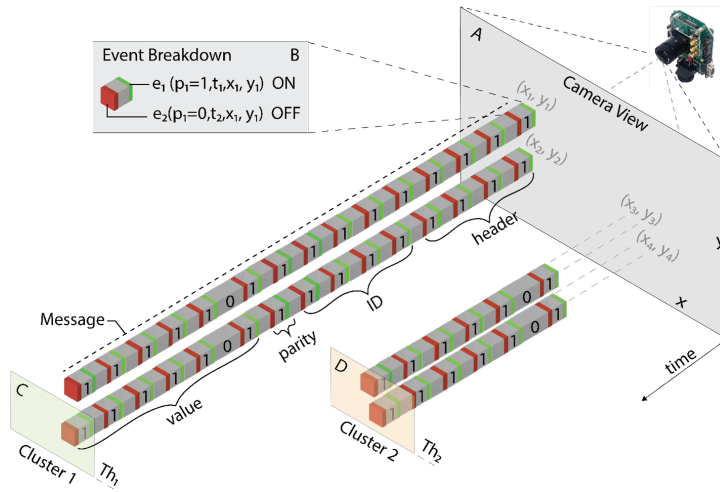


Fig. 5. Neuromorphic camera event decoding **A.** NeuroCamTag flashes an LED in OOK manner to create events which arrive in the camera’s view **B.** Polarity changes are decoded as on/off events. **C.** Similar messages are clustered by location using a time threshold based on the length of nearby messages to eliminate duplicates.

5 Analog NeuroCamTag System Overview

Focused on fulfilling design goal D3, which emphasizes adaptability and eliminating the need for device programming, we developed an analog NeuroCamTag utilizing a 555 timer with expandable slots for solar panels to adapt to varying light conditions. Unlike digital circuits that represent information using binary (0s and 1s), analog circuits represent information through frequency modulation. This approach allows for "programming" the circuits by adjusting passive elements like resistors and capacitors, directly supporting our D3 design objective. We also highlight that we aim to support D4 (low-cost and minimum components) with our analog NeuroCamtags, as they require only eight components.

Finally, recent advances in backscatter analog techniques [4], greatly inspired our design. In particular, using ultra-low-power oscillators for frequency-modulated sensing wireless communication of audio as well as resistance based sensors. While existing designs use it for backscatter, we use oscillator circuits for light based frequency modulation.

On the camera side, we capture the frequency of the LED blinks, which correspond to the transmitted FM signal from the analog NeuroCamTag. To isolate and extract FM signals from noise, a signal processing step is employed, filtering based on the intended signal bandwidth. Following this filtering process, the signal is segmented into discrete windows, allowing for the extraction of key features that can be harnessed to train a Machine Learning (ML) model for activity recognition.

5.1 Circuit Implementation

Energy Harvesting and Management: Similar to our digital tag, the analog counterpart uses solar panels (SM141K06L) for self-sustaining power. The analog tag employs frequency modulation (FM), runs continuously, and supports power-intensive sensors like microphones, leading to customizable sizes. For example, a microphone-equipped tag needs six solar cells and is post-it-note sized, while a light-dependent resistor version requires only two cells and is smaller. The analog NeuroCamTag offers flexibility with 2, 4, or 6 solar panels. This design

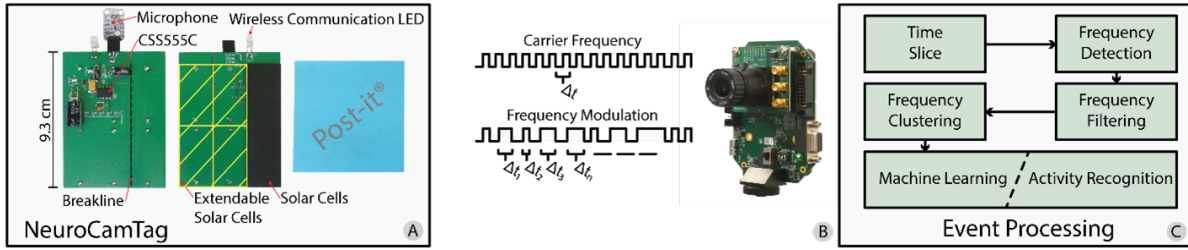


Fig. 6. Analog NeuroCamTag System Overview **A.** Battery-free wireless NeuroCamTag back and front view. **B.** Frequency modulated LED signal sent to camera **C.** Machine Learning, event processing pipeline that classifies activity.

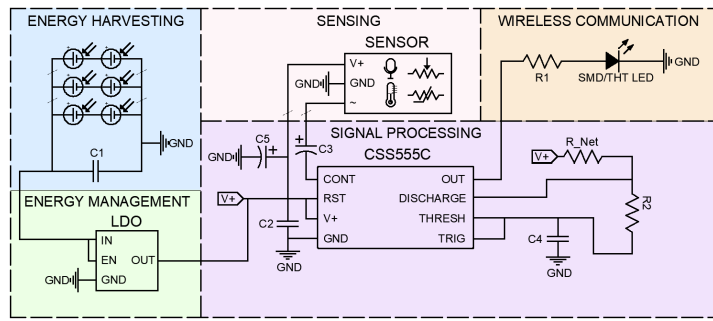


Fig. 7. Analog NeuroCamTag Schematic

flexibility led to the creation of the analog NeuroCamTag, featuring break lines on our PCB (refer to Figure 6A), allowing for configurations with 2, 4, or 6 solar panels.

Power from solar panels goes to a Low-Dropout Regulator (LDO) TPS7A0333DBVR with ultra-low quiescent current (IQ) of 200nA, ensuring signal stability. Each LDO port connects to a 1000 μ F ceramic capacitor for a fixed 3.3-volt output.

555 timer oscillator and sensors: The output voltage from the Low Dropout (LDO) regulator is applied to an astable-multivibrator circuit using a 555 timer, which acts as a resistance-to-frequency converter. We utilized a CSS555 timer, an ultra-low power timer that consumes a minimal 5 μ A at 1.2 V. This timer is part of a resistor-capacitor network consisting of resistors R1 and R2 and capacitor CT. The circuit generates oscillations at a specific carrier frequency and duty cycle, determined by the following relationship:

$$\text{Oscillation Frequency : } f = \frac{1.44}{((R1 + 2 \times R2) \times CT)} \quad (2)$$

$$\text{Duty Cycle: } D = \frac{(R1 + R2)}{(R1 + 2 \times R2)} \quad (3)$$

The carrier frequency and duty cycle are inversely proportional to the values of R1, R2, and CT. Lower values of these components yield higher frequencies and shorter duty cycles, whereas higher values result in lower frequencies and longer duty cycles. These component values (R1, R2, and CT) can be customized on our PCB (Figure 7), allowing the creation of new tags with distinct carrier frequencies or "IDs." This customization supports

the identification of multiple tags operating on a different carrier frequency. We tested $R_1=4M\Omega$, $R_2=470K\Omega$ and $C_T=1nF$ for a carrier frequency of 270Hz for the microphone tag.

In our circuit design (see Figure 7), the input signal to the Control Voltage (CV) pin of the timer modulates the output frequency and duty cycle. This modulation depends on the characteristics of the signal applied to the CV pin. Various sensors, such as microphones, light-dependent resistors, or pressure sensors, can be connected to this pin. They produce a frequency-modulated (FM) voltage signal at the output of the timer, which is then transmitted through an LED with a resistor, sending out the FM signal.

5.2 Software for Demodulating Analog NeuroCamTags

Similar to digital NeuroCamTag, an analog NeuroCamTag's LED blinks generate events with a polarity that indicate either ON or OFF states, triggered by changes in brightness from the tag's LED (Figure 6B). The tag's frequency modulation dictates the frequency of these events, correlating to the LED signal's frequency. Our camera records these events, capturing their timing and XY coordinates accurately. To extract the events, we use our camera API; specifically, we set a time buffer of 2ms; this ensures all events captured within the 2ms are passed to further processing blocks in the software pipeline.

Frequency Detection, Clustering and Filtering: To process the events along with their XY coordinates, we first convert each event that is timestamped into frequencies and cluster the frequencies to reduce redundancies using an implementation that is similar to FrequencyCam [33]. We then use a series of low-pass and high-pass filters to extract the signal of interest. For instance, our analog microphone NeuroCamTag uses 270 Hz carrier and uses a bandwidth from 250 Hz - 2KHz to modulate and send data; therefore, we filter out other frequencies (Figure 6C). However, if an environment has other sensors, such as resistive sensors (such as potentiometers, sliders, and light dependent resistors), they can occupy other parts of the available spectrum such as above 2KHz or below 250Hz, and their bandwidth is customizable depending on the resolution of the device desired.

5.3 Activity Recognition & Machine Learning

We use machine learning to classify activities based on the FM signal received from our analog NeuroCamTag. In particular, we used our analog battery-free microphone tag (Figures 1 and 7) to capture audio and send FM data wirelessly to our machine learning pipeline. Upon receiving and demodulating the FM signal, we extract features from a sliding window of 4000 data points and compute the time domain and frequency domain features. For spectral features, we used a 128 point Fast Fourier Transform (FFT) overlapping 50% from the signal data window. In addition, we used TSFEL [5], a feature extraction toolbox, to create spectral features (e.g. continuous wavelet transform, quantiles, binned entropy and etc.) In total, 41 features were fed into the machine learning model.

Figure 8 shows a series of different activities and their associated retrieved spectrum content. Note the variations in the duration, frequency bands, and amplitudes (intensity of color) for each of the activities.

For the classification of activities and user interactions, we use a random forest classifier although, other models e.g., boosted trees or dense networks are compatible with our analog NeuroCamTags).

We ran our random forest classifier using *Gridsearch* [32] to systematically determine the number of estimators and the random forest criterion (gini, entropy or log loss). Gridsearch determined 60 as the optimal number of estimators and 'gini' as the optimal criterion. These parameters were cross validated 5 fold by mean to determine the desired parameters.

Due to the variations in environmental conditions and end-use (i.e., applications), we expect that the system will require an initial calibration to train the activity classifier when first installed. Based on our preliminary studies, we have observed that this calibration can be accomplished in just a few minutes. However, if there is a change in the device type (e.g., replacing a microwave) that operates at a different frequency than the previous device, an additional calibration may be necessary.

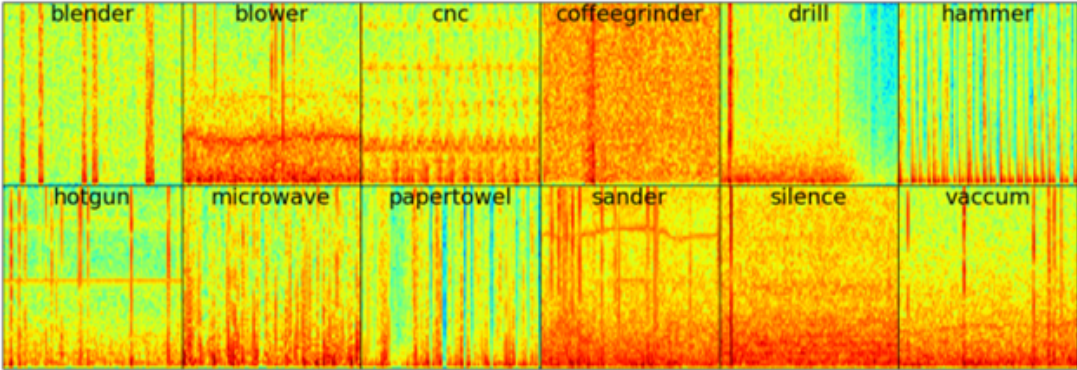


Fig. 8. Activity spectrograms from microphone equipped, sound encoded, analog NeuroCamTag

6 Technical Evaluation

In this section, we detail a series of experimental evaluations of our combined hardware and software system across several key dimensions. These explorations focus on 1) Analyzing how range, transmission speed, and accuracy impact our sensing devices, 2) Measuring the accuracy of message transmission at different angles of attack in our tags, 3) Examining the density limitations of tag placement, 4) Investigating how background interactions influence accuracy, and 5) Conducting various tests to confirm the power efficiency of our sensors.

Our accuracy tests were conducted primarily on digital tags, which communicate via binary data (sequences of 1's and 0's). In contrast, analog tags emit a continuous signal. For these, we assessed the detectability of their modulated carrier frequencies under varying conditions, such as different distances.

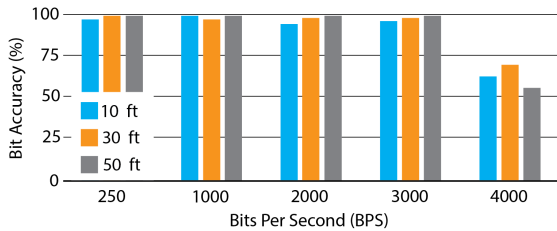


Fig. 9. BPS and message accuracy

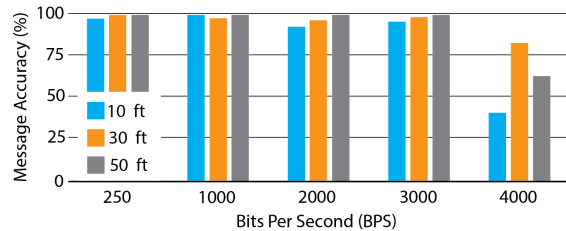


Fig. 10. BPS and bit accuracy rate

6.1 Experiment #1

Transmission Speed and Accuracy: To examine the range and transmission speed capabilities of our system, we implemented our digital NeuroCamTags encoding process, utilizing an LED device in the lab. We transmitted a 16-bit message (see §4.1) with varying identifiers corresponding to different transmission speeds: IDs of 0001, 0002, 0003, 0004 & 0005, representing speeds of 250, 1000, 2000, 3000, and 4000 BPS, respectively. Our testing involved moving our camera, equipped with decoding software, to distances of 10, 30, and 50 feet to gauge the decoding accuracy (see Figures 9 and 10). These distances were selected to mirror typical indoor room lengths. Our findings show a high message accuracy rate, exceeding 95% for all tested distances and speeds up to 3000 BPS. However, at 4000 BPS, accuracy notably decreased to below 75%, attributed to a hardware limitation in the camera's event processing capacity due to its readout architecture [33].

Table 1. Long Range Message and Bit Accuracy for through hole (THT) and surface mount (SMD) LED

Accuracy Type	LED Type	Distance	
		100 ft	200 ft
Message	SMD	95.0%	1.0%
	THT	90.0%	95.0%
Bit	SMD	97.4%	1.0%
	THT	89.8%	95.2%

Following our assessment of the message accuracy rate, we proceeded to analyze the bit accuracy rate. We attained a bit accuracy rate exceeding 97.6% at 3000 BPS, mirroring our message accuracy rate at this speed (Figure 10). However, as the transmission speed increased, the bit accuracy further declined. At 4000 BPS, we observed a bit accuracy rate of 62.7%, equivalent to approximately 10 bits received per 16 bits transmitted.

Analog Accuracy Experiment: As previously discussed, for analog tags, we conducted basic tests to detect modulated carrier frequencies of 300Hz, 1000Hz, and 2000Hz, the latter being the upper limit of our range. Our observations confirmed that these frequencies were successfully received using our demodulating software and demonstrated similar data throughput and range as the digital tag.

6.2 Experiment #2

Long Range and Accuracy Experiments: After establishing the maximum operating speed of our devices, we then tested their transmission range limits. We selected two extended distances of 100 feet and 200 feet for this purpose, with 200 feet being the maximum distance manageable in our indoor environment. At these distances, we implemented our message encoding and decoding software. We also explored the effect of LED type on transmission characteristics by comparing surface mount device (SMD) LEDs (part number IN-P32AT5UW) and through-hole (THT) LEDs.

The results were quite significant. At 100 feet, the THT LED sustained an impressive message accuracy rate of 90%. This is close to the SMD LED, whose accuracy was 95%. At 200 feet, the THT LED continued to maintain its accuracy level, but the SMD LED's accuracy fell to 1% (see Table 1). This difference in performance is primarily due to the higher microcandela (mcd) value of THT LED, which is 35,000 mcd, as opposed to the 1,000 mcd of the SMD LED. Because the neuromorphic camera operates by detecting changes in light's contrast, as the LEDs' distance from the camera increases, their mcd values diminish, leading to a decrease in contrast and, subsequently, impacting the transmission accuracy.

6.3 Experiment #3

Angle between Camera and Tag: Following our initial insights into the long-range capabilities of THT LEDs, we were motivated to explore further the dynamics of our system. We particularly focused on how the accuracy of message transmission interacts with the angle of attack and the type of LED. This led us to conduct another set of experiments that focus on these variables.

In these tests, we broadcast messages while varying the camera's position across different angles and distances. This setup allowed us to run our decoding pipeline under diverse conditions. The results, presented in Figure 11, reveal the accuracy of the message for both THT and SMD LEDs at distances of 10 and 50 feet and at angles from directly facing the sensor (0°) to nearly sideways (85°). In particular, at a 90° angle, neither type of LED was visible to the neuromorphic camera, and hence, 90° is not included in our analysis.

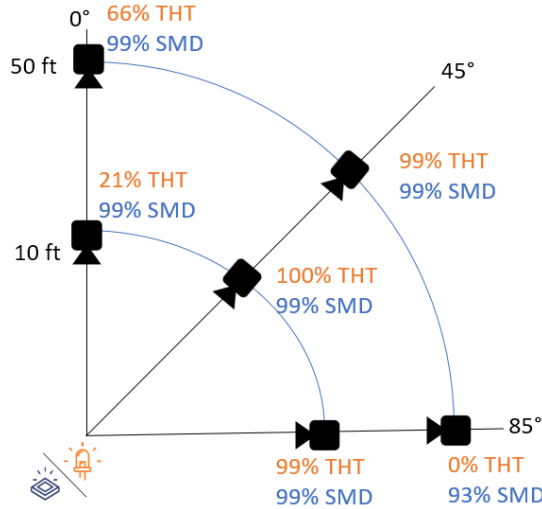


Fig. 11. Message accuracy (%) at different camera to LED viewing angles. THT: Through Hole LED (orange), SMD: Surface Mount Device (blue)

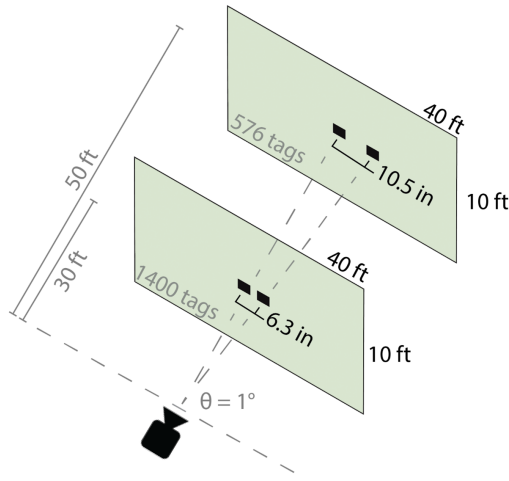


Fig. 12. Conceptual number of tags placed 1° apart on a 40' by 10' wall at 30' and 50' distance from camera.

Our tests revealed that the SMD LED delivered steady and reliable performance across all angles and distances tested. It was particularly effective at right angles of 0° and 90°, maintaining an accuracy rate of over 90%. This high level of consistency is likely due to the SMD LED's broad viewing angle of 120 degrees, which is significantly wider than the 15-degree viewing angle of the THT LED. Meanwhile, at a moderate angle of 45°, both the THT and SMD LEDs showed commendable performance, achieving accuracy rates of 99% and above.

6.4 Experiment #4

Contrast Effect on Accuracy: Neuromorphic cameras function by detecting changes in light contrast, prompting us to test two distinct background colors, white and black, to assess their impact on our tag design. In our experiment, we positioned an LED against either a solid white background (using copy paper) or a dark background (black poster board) and then transmitted our message. The camera was relocated to various distances (10 feet, 30 feet, and 50 feet) for testing, and we operated our message decoding software in different lighting conditions (with lights on and off). As Table 2 indicates, a dark black background provides consistently high recognition accuracy in indoor settings. Consequently, we suggest placing our tags against darker backgrounds for optimal performance.

6.5 Experiment #5

Distance Between Tags: To investigate the proximity limits for placing NeuroCamTags while maintaining high message accuracy, we positioned two tags at various angles relative to the camera. This setup allowed us to control their separation distances. We simultaneously broadcasted messages from these tags and then analyzed the decoded outputs. The separation distance between the tags was dictated by their angular distance in relation to the camera. For instance, at a 1° angle, as shown in Figure 12, the tags were 6.3 inches apart at 30 feet and 10.5 inches apart at 50 feet. We tested angles of 0.1°, 0.5°, and 1°, with the results detailed in Table 3, to identify the minimum viable distance between tags while maintaining high message accuracy.

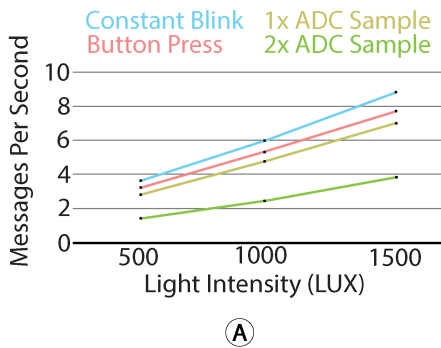
Table 2. Message accuracy with different LED background contrast.

		Dark BG	White BG
10 Feet	Ambient light	99%	76%
	No light	99%	93%
30 Feet	Ambient light	97%	75%
	No light	100%	100%
50 Feet	Ambient light	99%	20%
	No light	100%	100%

Table 3. Message accuracy at different degree separation between tags.

Distance (ft)	Degree of Separation		
	0.1°	0.5°	1.0°
30	58.9%	80.7%	91.1%
50	58.9%	73.3%	85.6%

Our results demonstrated that message accuracy remained above 90% at 30 feet and exceeded 85% at 50 feet with a minimum angular separation of 1° between tags. These overall tag density measurements were calculated considering a 70° horizontal camera field of view. Additionally, Figure 12 illustrates the feasible tag density on a 10'x40' wall at distances of 30 and 50 feet, assuming a 1° angular separation between tags. Based on these findings, we estimate the capacity to place approximately 1400 tags on a 40-foot wall at 30 feet and around 578 tags at 50 feet.



Solar Panel Configuration	Light Intensity (LUX)	
	Microphone	Resistive Sensor
2 In Series	2100	1000
3 In Series	1500	600
2 Parallel Sets Of 2 In Series	1200	400
3 Parallel Sets Of 2 In Series	800	350

Fig. 13. Power characteristics for NeuroCamTag A. Blink frequency for the digital tag in different light intensities. B. Minimum required light intensity for the analog tag in different solar panel configurations.

6.6 Experiment #6

As previously mentioned, to ensure interactivity (e.g., continuous user interaction through buttons, knobs, etc.), it's essential to transmit multiple messages per second. This not only minimizes errors but also maintains responsiveness. Given our message length of 16 bits and the Size, Weight, Power, and Cost (SWaP-C) limitations of our tags, we aimed to assess the power requirements for sensing and broadcasting multiple messages and determine the optimal transmission speed (BPS).

Operational Power Budget of Digital tag: As a first step, we measured the operational power needed for digital NeuroCamTags under various lux conditions. We measured this by using the Nordic Power Profiler Kit II as a power meter across the singular solar panel that charges our digital NeuroCamTag. The NeuroCamTag was made to run the *constant blink* program at 3000 BPS and would broadcast a message consisting of all 1's. The messages per second would be set so that the average power expended during operation would equal the average

Table 4. Energy expense to send a digital message at different BPS by various sensors.

BPS	Message Type			
	Constant	Button	Read	Read
	Blink	Press	1 ADC	2 ADC
500	85.4 μ J	90.2 μ J	100.9 μ J	175.7 μ J
1000	49.4 μ J	53.9 μ J	55.3 μ J	102.4 μ J
2000	25.4 μ J	26.8 μ J	28.2 μ J	53.9 μ J
3000	13.6 μ J	13.8 μ J	15.9 μ J	30.1 μ J

Table 5. Cold Start Time In Different Lighting Environments

Capacitor	Cold Start Time		
	1500 LUX	1000 LUX	500 LUX
680 μ F 16V	47 s	1.8 min	3.9 min
2200 μ F 6.3V	2.5 min	6.8 min	12.3 min
4400 μ F 6.3V	4.8 min	12.0 min	22.8 min
0.047 F 5.5V	52.8 min	2.3 hr	4.5 hr
0.25 F 5.5V	3.6 hr	7.8 hr	15 hr
0.5 5.5VF	6.7 hr	18.3 hr	34 hr

power delivered by the solar panel, see Figure 13. Our results are as follows: at 1500 lux, digital tags operated with 360 μ W of power; at 1000 lux, they operated with 260 μ W of power; and at 500 lux, they operated with a mere 65 μ W of power.

Power per Sensing Type: We also performed a power analysis on four key input sensing methods expected to be supported by our digital NeuroCam tags. These methods include constant blinking (for purposes like ID and pose tracking), button presses (applicable in game controllers, reed switches, etc.), reading one ADC (suitable for temperature sensors, sliders, etc.), and reading two ADCs (for joysticks, operating dual sliders, etc.). As discussed in the section on MCU and Computation (see §4.1), it's noted that buttons function in a low-power mode 4 (LPM4), while other input types oscillate between low-power mode 3 (LPM3) and the active mode due to the requirement of an auxiliary clock for ADC Reads. We used the Nordic Power Profiler Kit II to measure energy consumption from MCU wakeup to sleep mode, capturing characteristics like ADC initiation, button press power, and BPS.

Our evaluation of the power cost per message for sensing and transmitting data is presented in Table 4. We experimented with varying message transmission rates, including 500 BPS, 1000 BPS, 2000 BPS, and 3000 BPS. We performed our analysis at 3000 BPS, which was the highest speed/accuracy that still allowed for high accuracy (see §6). The results indicate that a transmission speed of 3000 BPS was the most power-efficient across all input sensing types.

Lux vs Message Rate vs Sensing Type: After determining that 3000 BPS is the most energy-efficient transmission speed, our next task involved assessing the number of messages that digital tags could transmit under varying light conditions, ranging from 500 lux (low light) to 1500 lux (bright environments). We conducted this evaluation for our four input sensing methods: constant button, button press, 1ADC, and 2ADC. In this experiment, we adjusted the device's message rate until it reached a stable capacitor voltage in different lighting scenarios.

Our findings, as depicted in Figure 13A, indicate that at the lowest light level of 500 lux, we were able to detect and transmit multiple messages for both button presses and constant blinking. In moderate light conditions, ranging from 500 to 1000 lux, we successfully achieved the sensing and transmission of 3-5 messages per second for all input types except for 2ADC. In brighter settings, exceeding 1000 lux, the rate increased to 5-8 messages per second for all conditions, again except for 2ADC. These results align closely with the energy consumption per message type observed in our prior studies.

Operational Power Budget of Analog Tag: Additionally, we investigated the relationship between lighting conditions and the number of solar panels required for our analog tags to function optimally under various lighting scenarios. Table 13B presents the necessary configurations of solar panels corresponding to different lux levels. Given that the Analog tag operates in an "always on" mode, it has a higher power consumption. Presently,

our analog microphone tag includes an electric microphone with a gain amplifier, which consumes approximately 250 μ A, in addition to the 555 timer and the rest of the circuit components. Since our analog tags are adaptable to light conditions, their power budget is determined by the solar panels used. We characterize the power required to run these tags in different lux, as seen in Figure 13B.

Energy Storage vs Cold Start vs Capacity: Finally, we aimed to explore how the choice of energy storage (capacitors) impacts cold start times and tag energy life. We measured the time it took for the NeuroCamTag to start operating from a fully uncharged state, ranging from 0 to 3.9 volts on the storage capacitor, marking the beginning of the AEM10941's buck converter.

Our findings reveal that smaller capacitors have a quick 4-minute start-up time even under moderate lux (500) conditions, while larger capacitors have a longer cold start time. However, the trade-off is that smaller caps provide limited power during power failures compared to larger caps. This highlights the importance of selecting capacitors tailored to specific applications: smaller capacitors for intermittent systems like temperature probes or reed switches and larger ones for high-frequency interactions like joystick controllers or constant blinking ID tags.

7 Applications

We propose several interactive applications to demonstrate both digital and analog NeuroCamTags: 1) Sensors and Interactive Devices 2) Multi-user, Multi-tag applications, 3) Object Use Tracking in Smart Kitchen and 4) Object Use Tracking in Smart Workshop.

7.1 Sensors and Interactive Devices

Input Devices: Buttons, Sliders, Knobs and Joystick We developed a variety of rich input devices that incorporate NeuroCamTags. These include inputs such as pressing a button (as illustrated in Figure 14A), rotating a knob (Figure 14D), sliding a control (Figure 14C), and maneuvering joysticks across XY coordinates (Figure 14F). Each device utilizes the ultra-low-power MSP430 microcontroller unit (MCU) in the digital NeuroCamTag. This setup operates on an interrupt-driven basis, toggling between low-power states and an active mode. Specifically, the button-tagged device alternates between LPM4 and active state, whereas other input devices transition between LPM3 and active state. For input mechanisms like knobs and sliders, a basic resistive divider circuit is employed to monitor voltage changes through the ADC, broadcasting the voltage at a rate of 3000 BPS. This process occurs at an optimized frequency of 7 messages per second, ensuring the system remains sufficiently responsive for quick human interactions. In the case of the joystick input device, the tag is activated from LPM3 to first measure and transmit the ADC value for the 'x' axis, then pauses briefly for 5ms before measuring and transmitting the 'y' axis ADC value. This approach effectively tracks both axes of the joystick, maintaining a practical transmission rate of nearly 4 messages per second.

Interactive Sensors: We also provide a variety of interactive sensors designed to monitor smart environments. For example, in workshop or kitchen settings, our temperature sensors (illustrated in Figure 15) can detect temperature changes. Utilizing reed switches, we have developed an application for monitoring supply levels (Figure 16B). This system records each interaction, keeps track of inventory, and sends out wireless notifications when restocking is needed. Additionally, we have equipped smart moisture sensors (Figure 14B) to monitor the soil moisture around plants, using ADC readings from the MCU on our digital tags for wireless communication. The moisture data transmitted is compared against a pre-defined soil moisture threshold and alerts the user depending on needs. Additionally, we have incorporated pressure sensors in our tags, which are designed to log and monitor pressure as recorded by users.

Multiple User, Multi Tag Applications We demonstrate in Figure 16 our system's capability in managing interactions from multiple users concurrently engaged in a game of 'tic-tac-toe'. This interaction is facilitated

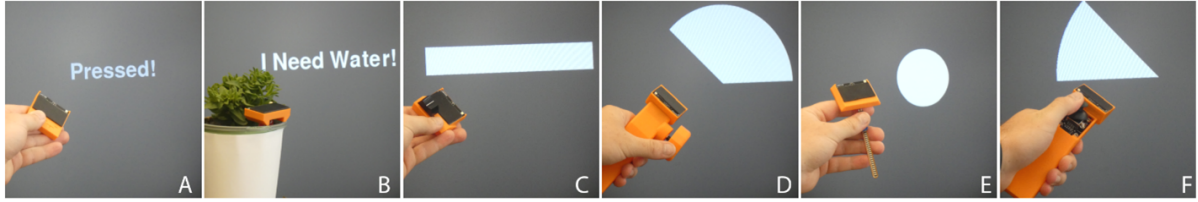


Fig. 14. Applications of digital NeuroCamTag A. Button Press B. Soil moisture C. Linear slider D. Rotary knob E. Pressure sensor F. Joystick controller

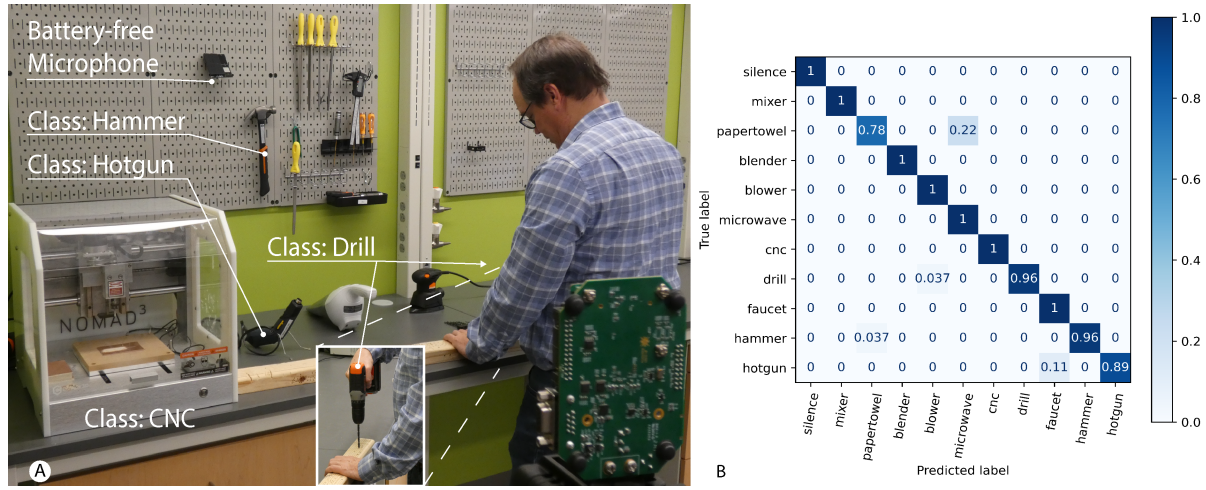


Fig. 15. Occlusion aware environment sensing A. Battery-free microphone modulated LED signal sent to neuromorphic camera in a workshop environment. B. Confusion matrix accuracy (%) for classes in the kitchen and the workshop.

using two analog NeuroCamTags, each set to a unique carrier frequency that corresponds to specific display colors. Our system decodes these frequencies along with their locations to map them on the display, enabling each player to simultaneously draw on the screen in their distinctive colors.

Figure 2B depicts a pong game with two users employing the digital NeuroCamTag model pictured in 14D. Here, each game controller incorporates a tag assigned with a distinct "ID." This unique identification allows the system to accurately distinguish and process the signals emitted from the rotary sensors in each controller.

7.2 Smart Environments - Kitchen & Workshop

Using our battery-free analog and digital NeuroCamTags, we have created a smart kitchen and workshop environment, as illustrated in Figure 15. In both the kitchen and workshop, we deployed temperature sensors, reed switches, and a microphone tag.

Sensors We employed a temperature sensor on the oven (Figure 1) to monitor its temperature in the kitchen and on a hot glue gun (Figure 2) in the workshop. Reed switches were utilized to track the usage of kitchen drawers (1). Additionally, our analog microphone tag was deployed in both environments to monitor and predict activities using the previously described machine learning (ML) pipeline. The system enables us to track and predict the usage of various objects in both the workshop and the kitchen.

Activity Recognition The analog NeuroCamTag system was deployed for recording data from both the kitchen and the workshop. Notice in our workshop environment (Figure 15), that even though the user activity is occluded, our system can still pick up audio data. We collected data for eleven activities: Microwave, Faucet, Blender, Mixer, Vacuum, Blower, CNC, Drill, Hammer, Hot Air Gun, and Silence. During raw data collection by the Neuromorphic Camera, only one object was active at a time. Each activity was recorded twice, with a duration of 120 seconds for each recording. The machine learning model was trained on data collected over three different days, with each day's sessions having distinct lighting conditions to ensure the model's robustness.

The NeuroCamTag machine learning model evaluation utilized a leave-one-out cross-validation method by collecting a separate, never-used dataset. The analog NeuroCamTag system demonstrated an average classification accuracy of 96.3% across various objects in specific locations and diverse ambient light conditions. Notably, the false positive rate remained low at 1.3%. Specific details regarding classification rates for each object are detailed in the confusion matrix (Figure 15). For example, the misclassification of a "hot gun" as a "faucet" exhibited a false positive rate of 11%. Similarly, the misclassification of a "drill" as a "blower" exhibited a false positive rate of 3.7%. These observations shed light on the system's behavior in specific recognition scenarios, indicating areas for potential refinement and further investigation.

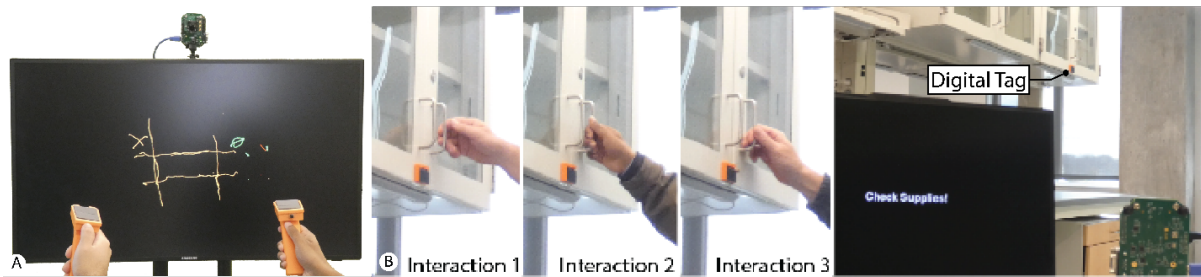


Fig. 16. Multi-user interactive controls demo **A.** Analog NeuroCamTag playing Tic-Tac-Toe **B.** Digital NeuroCamTag reed switch monitoring cabinet access

7.3 Long-Term Deployment Study: Kitchen

7.3.1 Procedure. We used three digital NeuroCamTags in a kitchen setting from Figure 1, featuring two drawer monitoring tags (reed switch) and one toaster monitoring tag (temperature sensing). The location mimicked actual real-world deployment and NeuroCamTags were used in an everyday setting. The lowest lux measured throughout the experiment was 746 lux. Our system was deployed for 144 hours, and one experimenter visited it several times each day. Each of the digital tags was configured to broadcast every second at 3000 bps. During each visit, one or multiple tasks were performed, such as opening a drawer and/or turning on the toaster to either the 'toast' setting or the 'warm' setting. The task, time, and duration were recorded manually to establish ground truth interactions. Additionally, the start temperature and peak temperature were recorded using an AMES infrared thermometer.

7.3.2 Results. Figure 17 shows each device's status for the 6-day period. Over the 6-day period, over 2,000,000 data points were collected. The 36 ground truth operations were compared to the recorded data, 100% of actions were detected. Additionally, as seen in Figure 17, the toaster temperature monitor recorded both the temperature of the toaster during use and ambient temperatures when it was not in use. Also, while there were only 36 actions, the drawer sensor can detect how long the drawer was open (from close to open to close).

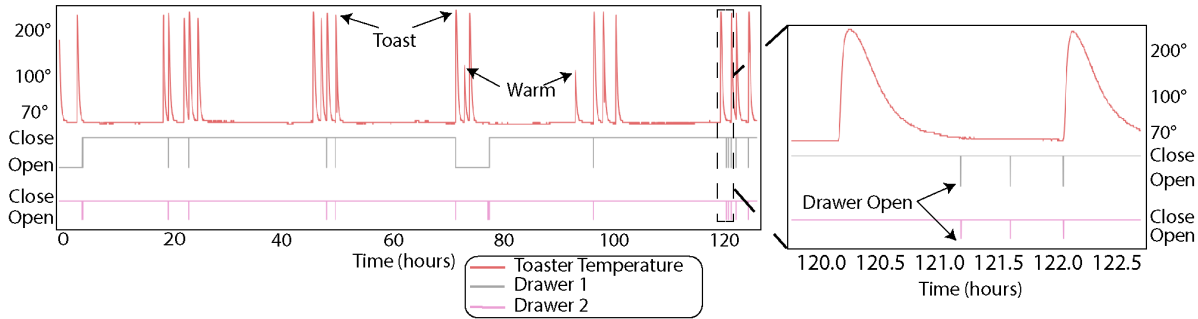


Fig. 17. Multiple event distribution over time of three NeuroCamTags deployed over a 6-day period. The events show the continuous operating nature of the tags sensing activities, which include using a toaster oven and opening/closing drawers.

8 Discussion

In this section, we compare our work and discuss the advantages over existing work in two key areas: visible light communication (VLC) based sensing systems and battery-free RF sensing.

8.1 Visible Light Communication and Sensing

In the field of visible light communication (VLC) based sensing systems, a wide array of research has significantly advanced the technology. Schmid et al. [44] initially developed an LED to LED VLC system, achieving data transmission over 2 meters at 800 b/s utilizing 289 mW, and later enhanced this with an IoT VLC system [45] using PWM ON-OFF Keying for up to 400 b/s transmission. Additional work in low-power communication technologies includes Xu et al. [57], who developed Passive VLC in 2017, noting a power consumption of 150 μ W and achieving a range of 4.5 meters. Additionally, the RetroVLC system, with a power consumption of 90 μ W, demonstrated effective communication over distances of up to 2.4 meters [24]. Wu et al. [55] introduced RetroTurbo, which reached 7.5 meters and consumed 0.8 mW transmitting up to 8 kbps. Xu et al. [56] built RetroMUMIMO and investigated concurrency in visible light backscatter communications (VLBC) to reach 3.75 meters using 0.2 mW emphasizing reflective architectures. LightAnchors [1], closely aligned with our research, utilized advancements in slow-motion cameras, such as the iPhone 7's 240 fps feature, to detect point light LEDs in a scene. Though effective, LightAnchors relied on energy-intensive traditional RGB cameras that require constant operation for cue detection. In contrast, our works novel neuromorphic cameras, which are highly energy-efficient (about 1mW) and capable of an impressive 4000 Hz (4000 FPS) data capture rate per pixel. This enables the simultaneous capture of multiple point light LED sources at high frame rates.

Moreover, our study showcases the capability for long-range battery-free sensing of user interactions (Figure 18), operating at a mere 65 μ W, even in low-light (500 lux) conditions, as detailed in the section on the operational power of the digital tag (Section §6.6).

8.2 Battery-free RF Interaction sensing

Battery-free wireless interactive sensing systems come in two categories: those that require instrumentation of objects with tags such as RFID [42] and those that take advantage of wireless signals around us such as Wi-fi, mmWave, etc not requiring labels and use RF reflection from human/object movement to detect interaction. We now go over a brief overview of these works.

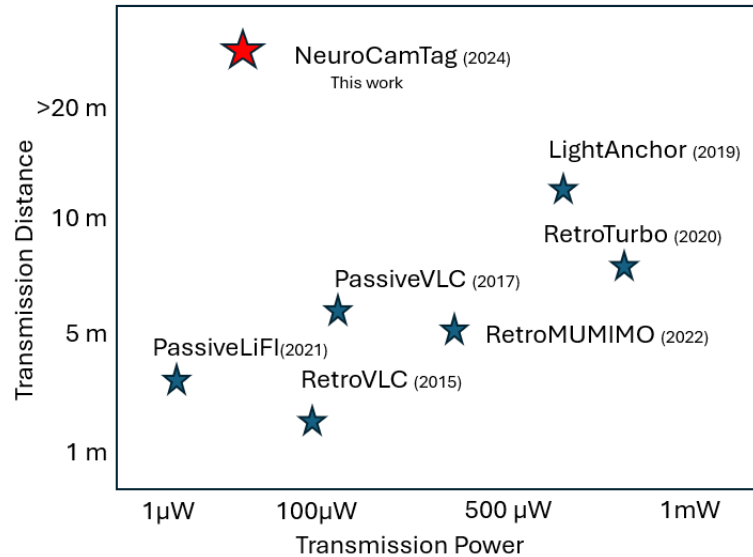


Fig. 18. Distance and power comparison of recent Visible Light Communication (VLC) technology [1, 24, 28, 55–57]

8.2.1 Tag-based RF Sensing approaches: To provide battery-free RF sensing, the tagging based approach relies on designing tags that harvest ambient energy from the environment to wirelessly communicate about interaction. There is a need to balance energy harvesting from environmental or human interactions with power efficiency, functionality, circuit complexity, and form factor. Amongst tag-based RF Sensing approaches is Wang’s LightSign [53], which combines VLC with RFID adding a photodiode to an RFID circuit to enhance tag localization, but are range limited due to light power requirement.

The first battery-free wireless sensors are rooted in RFID tags like WISP [42, 51] and Moo [31]. They featured programmable tags with onboard sensors wirelessly communicating via radio frequency backscatter. This led to the development of a hybrid analog-digital modulation scheme using WISP [48] for transmitting acoustic data. RFID based sensor advancements were furthered in PaperID [21], RapID [47], ID sense [23], LiveTag [15], and RF Bandaid [39], extending to touch interactions and multi-touchpoint detection. Similar to RFID backscatter mechanisms, other Wifi-based backscatter tags [60], mmWave based backscatter tags [27] have also been proposed for on-body sensors and environmental monitoring, respectively.

Finally, RF tags have also focused on purely analog communication [3, 28, 40, 61] due to their simplicity and power efficiency. For example, Ranganathan et al. [39] demonstrated RFBandaid operating at $160\mu\text{W}$ with a range of 9 meters. Although all these advancements are notable, most of the aforementioned RF tag based sensing technologies have a limited range of 12m.

Recent advances such as Lorea [52], Lora Backscatter [49] tags have extended these ranges to several hundred meters. For an in-depth analysis of the relationship between range and input power at the transmitter, we direct the readers to the work of Ranganathan et al [40] (see Figure 9 in that paper).

Furthermore, there is an array of non-backscatter communication techniques, i.e., active communication, in the realm of battery-free sensors that offer extended range but at the cost of increased energy. This category encompasses straightforward sense-and-transmit sensors powered by ambient energy, these include systems that use, energy-harvesting, and commodity radio communication technologies such as low-power BLE.

For instance, Fraternali et al. introduced Pible in 2018, harnessing BLE Advertising with a power consumption of 648 μW [11]. Jeon's luXbeacon, operating on the nRF51822 platform, offers a power-efficient solution with an estimated range of approximately 100 meters [20]. Similarly, Saoda et al. developed Herald in 2019, boasting a power consumption of 200 μW and a similar range estimation [43]. Yang et al. [59] created Minikers, tags that harvest kinetic energy from human interaction to actuate devices such as opening blinds and communicate via BLE.

8.2.2 Tag-free RF Sensing approaches: Unlike NeuroCamTag, which uses a physical tag, tag-free sensing exists and uses RF to communicate, locate and identify gestures, poses and activities. Several RF-based systems leverage WiFi for activity recognition [25, 38, 41] and some use mmWave [58, 62] for activity recognition.

8.2.3 Comparison to existing RF sensing approaches: Our work has several advantages over RF-based approach in general. First, NeuroCamTags is based on visible light and thus completely immune to the interference from RF spectrum, which is already crowded with “default” LAN and WPAN technologies such as WiFi, BLE. Second, because of the backscattering nature, some of the aforementioned RF-based systems tend to expose their transmissions to a wide surrounding area, leaving a good chance for side readers to overhear the information being transmitted. In contrast, NeuroCamTag relies on VLC, where signals are confined within a physical space and cannot penetrate walls, providing better security and privacy compared to RF signals. Through the use of highly directional LEDs, we can further constrain the uplink transmission to stick along the tag-reader path. Overall, NeuroCamTag has good security properties, while other RF systems have to enhance their security with extra efforts (padding, delaying packets, or injecting dummy traffic) [6]. Additionally, by leveraging physicality of the NeuroCamTags can provide agency to users to control privacy. For instance, using tape to cover the LED makes for a more cost effective means of privacy [9]. Finally, VLC systems do not cause electromagnetic interference like RF systems, making them suitable for use in sensitive environments like hospitals, etc. where sensors need to be deployed and non-interference to RF medical devices is crucial. Similarly, in environments that produce high EMI, like factories with heavy machinery, NeuroCamTags could ensure reliable machine-to-machine sensing and communication.

9 Limitations & Future Work

Power: Further power optimization could be a future goal. For instance, our current implementation of the analog tag is not optimized to run in the ultra-low-power mode of the CSS555 timer. The timer can run under 5 μA by reprogramming the EEPROM. Furthermore, LDOs such as the TI TPS7A0328DBVR, which operate at lower voltage levels, are available to further reduce the power budget for analog tags. Likewise, the power consumption for operating microphones can be optimized through the utilization of an ICS-40310 MEMS microphone, capable of running on a 1V supply and consuming as little as 16 μA of current, all while delivering a 64dB SNR. Similarly, other ultra-low power MCUs like the Apollo4 [50] could be explored for Digital NeuroCamTags.

Additional Energy Harvesting Techniques: The current implementation of our tags operates solely on ambient solar power. However, future iterations of NeuroCamTags could utilize alternative sources such as harvested piezoelectric, thermal, motion, etc. Prior research [26, 63] has explored various sources that are opportunistically available in the built environment.

Modulation and Error Correction techniques: Additional modulation techniques such as phase shift keying (PSK) could be explored and might improve the ability of our system to pick up event transmissions even faster. However, they would require additional changes to the camera sensor’s hardware and software. Finally, lightweight error correction techniques such as hamming codes could be explored by increasing the parity bits.

Line of Sight Operation: Due to the directional nature of light, NeuroCamTags inherently benefit from enhanced security, such as being resistant to eavesdropping. However, it also faces a fundamental limitation, shared by all visible sensing and communication systems, in that it cannot function in non-line-of-sight scenarios.

Direct Edge Sensing and Multi-class predictions

As we continue to develop NeuroCamTags, effectively managing complex computational tasks becomes essential away from the edge and in centralized processing environments. Our current setup, which includes the analog audio tag, does not utilize on-device machine learning; instead, it relies on centralized processing near the camera. This approach allows us to leverage algorithms that require greater computational power than edge devices typically provide.

A significant opportunity for future enhancement is the ability to detect multiple active devices simultaneously—a challenge often referred to as polymorphic multi-classification [30]. While our system currently employs classical machine learning techniques for single-class detection, expanding to use dense neural networks (DNNs) for multi-classification tasks could be possible because of the computational power available away from the edge. This progression would enable more sophisticated and responsive interactions in smart environments, taking full advantage of the computational capabilities available near the camera.

10 Conclusion

With our work on NeuroCamTags, we demonstrate a novel approach to enable battery-free, long-range wireless sensing utilizing neuromorphic cameras. We demonstrate through technical evaluations the robustness of our approach with respect to sensing at long distances as much as 200 feet across a variety of lighting conditions, including low light (500 lux) and across wide placements in an environment. We demonstrate a range of rich interactive sensing opportunities with NeuroCamTags, including battery-free input devices such as buttons, sliders, and knobs, with multiple multi-user application devices. Furthermore, we demonstrate the ability of the NeuroCamTag system to monitor using up to 11 objects in two smart environments (a kitchen and a workshop) with a high activity recognition accuracy of 96.3%. Our techniques enable a rich interaction application space for HCI researchers with a focus on creating battery-free and eco-friendly intelligent environments.

Acknowledgments

We thank all the reviewers for their insightful feedback on improving this paper. We also appreciate the valuable suggestions, feedback, and initial efforts from Hasibul Alam, Christian Tongate, and Adithya Sastry.

References

- [1] Karan Ahuja, Sujeath Pareddy, Robert Xiao, Mayank Goel, and Chris Harrison. 2019. LightAnchors: Appropriating Point Lights for Spatially-Anchored Augmented Reality Interfaces. In *Proceedings of the 32nd Annual ACM Symposium on User Interface Software and Technology* (New Orleans, LA, USA) (*UIST ’19*). Association for Computing Machinery, New York, NY, USA, 189–196. <https://doi.org/10.1145/3332165.3347884>
- [2] Arnon Amir, Brian Taba, David Berg, Timothy Melano, Jeffrey McKinstry, Carmelo Di Nolfo, Tapan Nayak, Alexander Andreopoulos, Guillaume Garreau, Marcela Mendoza, et al. 2017. A low power, fully event-based gesture recognition system. In *Proceedings of the IEEE conference on computer vision and pattern recognition*. IEEE, Hawaii, USA, 7243–7252.
- [3] Nivedita Arora and Gregory D Abowd. 2018. ZEUSSS: Zero energy ubiquitous sound sensing surface leveraging triboelectric nanogenerator and analog backscatter communication. In *Adjunct Proceedings of the 31st Annual ACM Symposium on User Interface Software and Technology*. IEEE, unknown, 81–83.
- [4] Nivedita Arora, Ali Mirzazadeh, Injoo Moon, Charles Ramey, Yuhui Zhao, Daniela C. Rodriguez, Gregory D. Abowd, and Thad Starner. 2021. MARS: Nano-Power Battery-free Wireless Interfaces for Touch, Swipe and Speech Input. In *The 34th Annual ACM Symposium on User Interface Software and Technology* (*UIST ’21*). Association for Computing Machinery, New York, NY, USA, 1305–1325. <https://doi.org/10.1145/3472749.3474823>
- [5] Marília Barandas, Duarte Folgado, Letícia Fernandes, Sara Santos, Mariana Abreu, Patrícia Bota, Hui Liu, Tanja Schultz, and Hugo Gamboa. 2020. TSFEL: Time Series Feature Extraction Library. *SoftwareX* 11 (Jan. 2020), 100456. <https://doi.org/10.1016/j.softx.2020.100456>

- [6] Ludovic Barman, Alexandre Dumur, Apostolos Pyrgelis, and Jean-Pierre Hubaux. 2021. Every Byte Matters: Traffic Analysis of Bluetooth Wearable Devices. *Proceedings of the ACM on Interactive, Mobile, Wearable and Ubiquitous Technologies* 5, 2 (June 2021), 1–45. <https://doi.org/10.1145/3463512>
- [7] Guang Chen, Wenkai Chen, Qianyi Yang, Zhongcong Xu, Longyu Yang, Jörg Conradt, and Alois Knoll. 2020. A novel visible light positioning system with event-based neuromorphic vision sensor. *IEEE Sensors Journal* 20, 17 (2020), 10211–10219.
- [8] Daniel G Costa, Francisco Vasques, Paulo Portugal, and Ana Aguiar. 2020. On the use of cameras for the detection of critical events in sensors-based emergency alerting systems. *Journal of Sensor and Actuator Networks* 9, 4 (2020), 46.
- [9] Youngwook Do, Nivedita Arora, Ali Mirzazadeh, Injoo Moon, Eryue Xu, Zhihan Zhang, Gregory D Abowd, and Sauvik Das. 2023. Powering for privacy: improving user trust in smart speaker microphones with intentional powering and perceptible assurance. In *32nd USENIX Security Symposium (USENIX Security 23)*. USENIX, Anaheim, CA, USA, 2473–2490.
- [10] Anthony Ferrese. 2015. Battery Fundamentals. *GetMobile: Mobile Comp. and Comm.* 19, 3 (Dec. 2015), 29–32. <https://doi.org/10.1145/2867070.2867082>
- [11] Francesco Fraternali, Bharathan Balaji, Yuvraj Agarwal, Luca Benini, and Rajesh Gupta. 2018. Pible: battery-free mote for perpetual indoor BLE applications. In *Proceedings of the 5th Conference on Systems for Built Environments (BuildSys ’18)*. Association for Computing Machinery, New York, NY, USA, 168–171. <https://doi.org/10.1145/3276774.3282822>
- [12] Guillermo Gallego, Tobi Delbrück, Garrick Orchard, Chiara Bartolozzi, Brian Taba, Andrea Censi, Stefan Leutenegger, Andrew Davison, Jörg Conradt, Kostas Daniilidis, and Davide Scaramuzza. 2022. Event-based Vision: A Survey. *IEEE Transactions on Pattern Analysis and Machine Intelligence* 44, 1 (Jan. 2022), 154–180. <https://doi.org/10.1109/TPAMI.2020.3008413> arXiv:1904.08405 [cs].
- [13] Guillermo Gallego, Tobi Delbrück, Garrick Orchard, Chiara Bartolozzi, Brian Taba, Andrea Censi, Stefan Leutenegger, Andrew J Davison, Jörg Conradt, Kostas Daniilidis, et al. 2020. Event-based vision: A survey. *IEEE transactions on pattern analysis and machine intelligence* 44, 1 (2020), 154–180.
- [14] Guillermo Gallego, Tobi Delbrück, Garrick Orchard, Chiara Bartolozzi, Brian Taba, Andrea Censi, Stefan Leutenegger, Andrew J. Davison, Jörg Conradt, Kostas Daniilidis, and Davide Scaramuzza. 2022. Event-Based Vision: A Survey. *IEEE Transactions on Pattern Analysis and Machine Intelligence* 44, 1 (2022), 154–180. <https://doi.org/10.1109/TPAMI.2020.3008413>
- [15] Chuhan Gao, Yilong Li, and Xinyu Zhang. 2019. Livetag: Sensing human-object interaction through passive chipless wi-fi tags. *GetMobile: Mobile Computing and Communications* 22, 3 (2019), 32–35.
- [16] Vanessa Gray. 2021. *Let's rethink e-waste, and pave the way to a waste-free economy for electronics - ITU Hub*. Technical Report. ITU, 1211 Geneva 20 Switzerland. <https://www.itu.int/hub/2020/05/lets-rethink-e-waste-and-pave-the-way-to-a-waste-free-economy-for-electronics>
- [17] Ruiyi Guang, Xiang Li, Yaguo Lei, Naipeng Li, and Bin Yang. 2023. Non-Contact Machine Vibration Sensing and Fault Diagnosis Method Based on Event Camera. In *2023 CAA Symposium on Fault Detection, Supervision and Safety for Technical Processes (SAFEPROCESS)*. IEEE, Yibin, Sichuan, China, 1–5. <https://doi.org/10.1109/SAFEPROCESS58597.2023.10295762>
- [18] Josiah Hester and Jacob Sorber. 2017. The Future of Sensing is Batteryless, Intermittent, and Awesome. In *SensSys ’17: Proceedings of the 15th ACM Conference on Embedded Network Sensor Systems*. Association for Computing Machinery, New York, NY, USA, 1–6. <https://doi.org/10.1145/3131672.3131699>
- [19] Craig Iaboni, Himanshu Patel, Deepan Lobo, Ji-Won Choi, and Pramod Abichandani. 2021. Event Camera Based Real-Time Detection and Tracking of Indoor Ground Robots. *IEEE Access* 9 (2021), 166588–166602. <https://doi.org/10.1109/ACCESS.2021.3133533> Conference Name: IEEE Access.
- [20] Kang Eun Jeon, James She, Jason Xue, Sang-Ha Kim, and Soochang Park. 2019. luXbeacon—A Batteryless Beacon for Green IoT: Design, Modeling, and Field Tests. *IEEE Internet of Things Journal* 6, 3 (June 2019), 5001–5012. <https://doi.org/10.1109/JIOT.2019.2894798> Conference Name: IEEE Internet of Things Journal.
- [21] Keiko Katsuragawa, Ju Wang, Ziyang Shan, Ningshan Ouyang, Omid Abari, and Daniel Vogel. 2019. Tip-tap: battery-free discrete 2D fingertip input. In *Proceedings of the 32nd Annual ACM Symposium on User Interface Software and Technology*. ACM, New York, NY, USA, 1045–1057.
- [22] Beat Kueng, Elias Mueggler, Guillermo Gallego, and Davide Scaramuzza. [n. d.]. Low-latency visual odometry using event-based feature tracks. In *2016 IEEE/RSJ International Conference on Intelligent Robots and Systems (IROS)*. IEEE, 09–14. <https://doi.org/10.1109/IROS.2016.7758089>
- [23] Hanchuan Li, Can Ye, and Alanson P. Sample. 2015. IDSense: A Human Object Interaction Detection System Based on Passive UHF RFID. In *Proceedings of the 33rd Annual ACM Conference on Human Factors in Computing Systems (Seoul, Republic of Korea) (CHI ’15)*. Association for Computing Machinery, New York, NY, USA, 2555–2564. <https://doi.org/10.1145/2702123.2702178>
- [24] Jiangtao Li, Angli Liu, Guobin Shen, Liqun Li, Chao Sun, and Feng Zhao. 2015. Retro-VLC: Enabling Battery-free Duplex Visible Light Communication for Mobile and IoT Applications. In *Proceedings of the 16th International Workshop on Mobile Computing Systems and Applications*. ACM, Santa Fe New Mexico USA, 21–26. <https://doi.org/10.1145/2699343.2699354>
- [25] Jian Liu, Yan Wang, Yingying Chen, Jie Yang, Xu Chen, and Jerry Cheng. 2015. Tracking Vital Signs During Sleep Leveraging Off-the-shelf WiFi. In *Proceedings of the 16th ACM International Symposium on Mobile Ad Hoc Networking and Computing (MobiHoc ’15)*. Association

- for Computing Machinery, New York, NY, USA, 267–276. <https://doi.org/10.1145/2746285.2746303>
- [26] John Mamish, Amy Guo, Thomas Cohen, Julian Richey, Yang Zhang, and Josiah Hester. 2023. Interaction Harvesting: A Design Probe of User-Powered Widgets. *Proceedings of the ACM on Interactive, Mobile, Wearable and Ubiquitous Technologies* 7, 3 (Sept. 2023), 112:1–112:31. <https://doi.org/10.1145/3610880>
- [27] Mohammad Hossein Mazaheri, Alex Chen, and Omid Abari. 2021. mmTag: a millimeter wave backscatter network. In *Proceedings of the 2021 ACM SIGCOMM 2021 Conference (SIGCOMM '21)*. Association for Computing Machinery, New York, NY, USA, 463–474. <https://doi.org/10.1145/3452296.3472917>
- [28] Muhammad Sarmad Mir, Borja Genoves Guzman, Ambuj Varshney, and Domenico Giustiniano. 2021. PassiveLiFi: Rethinking LiFi for Low-Power and Long Range RF Backscatter. In *Proceedings of the 27th Annual International Conference on Mobile Computing and Networking* (New Orleans, Louisiana) (*MobiCom '21*). Association for Computing Machinery, New York, NY, USA, 697–709. <https://doi.org/10.1145/3447993.3483262>
- [29] Elias Mueggler, Basil Huber, and Davide Scaramuzza. 2014. Event-based, 6-DOF pose tracking for high-speed maneuvers. In *2014 IEEE/RSJ International Conference on Intelligent Robots and Systems*. IEEE, Chicago, Illinois, 2761–2768. <https://doi.org/10.1109/IROS.2014.6942940>
- [30] Kakali Nath and Kandarpa Kumar Sarma. 2024. Separation of overlapping audio signals: A review on current trends and evolving approaches. *Signal Processing* 221 (Aug. 2024), 109487. <https://doi.org/10.1016/j.sigpro.2024.109487>
- [31] University of Massachusetts Amherst. 2023. *UnichMOO*. University of Massachusetts Amherst. <https://github.com/spqr/umichmoo>
- [32] F. Pedregosa, G. Varoquaux, A. Gramfort, V. Michel, B. Thirion, O. Grisel, M. Blondel, P. Prettenhofer, R. Weiss, V. Dubourg, J. Vanderplas, A. Passos, D. Cournapeau, M. Brucher, M. Perrot, and E. Duchesnay. 2011. Scikit-learn: Machine Learning in Python. *Journal of Machine Learning Research* 12 (2011), 2825–2830.
- [33] Bernd Pfrommer. 2022. Frequency Cam: Imaging Periodic Signals in Real-Time. [https://doi.org/10.48550/arXiv.2211.00198 \[cs\]](https://doi.org/10.48550/arXiv.2211.00198)
- [34] Chiara Plizzari, Mirco Planamente, Gabriele Goletto, Marco Cannici, Emanuele Gusso, Matteo Matteucci, and Barbara Caputo. 2022. E2 (go) motion: Motion augmented event stream for egocentric action recognition. In *Proceedings of the IEEE/CVF conference on computer vision and pattern recognition*. IEEE, New Orleans, LA, USA, 19935–19947.
- [35] Prophesee. 2023. *Prophesee Announces Collaboration with Qualcomm*. prophesee.ai. <https://www.prophesee.ai/2023/02/27/prophesee-qualcomm-collaboration-snapdragon>
- [36] Prophesee.ai 2023. *Event-Based Vision Evaluation Kits | PROPHESEE*. Prophesee.ai. <https://www.prophesee.ai/event-based-evaluation-kits> [Online; accessed 15. Nov. 2023].
- [37] prophesee.ai 2023. *Event-Based Metavision Sensor GENX320*. prophesee.ai. <https://www.prophesee.ai/event-based-sensor-genx320/>
- [38] Qifan Pu, Sidhant Gupta, Shyamnath Gollakota, and Shwetak Patel. 2013. Whole-home gesture recognition using wireless signals. In *Proceedings of the 19th annual international conference on Mobile computing & networking (MobiCom '13)*. Association for Computing Machinery, New York, NY, USA, 27–38. <https://doi.org/10.1145/2500423.2500436>
- [39] Vaishnavi Ranganathan, Sidhant Gupta, Jonathan Lester, Joshua R. Smith, and Desney Tan. 2018. RF Bandaid: A Fully-Analog and Passive Wireless Interface for Wearable Sensors. *Proceedings of the ACM on Interactive, Mobile, Wearable and Ubiquitous Technologies* 2, 2 (July 2018), 1–21. <https://doi.org/10.1145/3214282>
- [40] Vaishnavi Ranganathan, Sidhant Gupta, Jonathan Lester, Joshua R. Smith, and Desney Tan. 2018. RF Bandaid: A Fully-Analog and Passive Wireless Interface for Wearable Sensors. *Proceedings of the ACM on Interactive, Mobile, Wearable and Ubiquitous Technologies* 2, 2 (July 2018), 79:1–79:21. <https://doi.org/10.1145/3214282>
- [41] Yili Ren, Zi Wang, Sheng Tan, Yingying Chen, and Jie Yang. 2021. Winect: 3D Human Pose Tracking for Free-form Activity Using Commodity WiFi. *Proceedings of the ACM on Interactive, Mobile, Wearable and Ubiquitous Technologies* 5, 4 (Dec. 2021), 1–29. <https://doi.org/10.1145/3494973>
- [42] Alanson P Sample, Daniel J Yeager, Pauline S Powledge, Alexander V Maminshev, and Joshua R Smith. 2008. Design of an RFID-based battery-free programmable sensing platform. *IEEE transactions on instrumentation and measurement* 57, 11 (2008), 2608–2615.
- [43] Nurani Saoda and Bradford Campbell. 2019. No Batteries Needed: Providing Physical Context with Energy-Harvesting Beacons. In *Proceedings of the 7th International Workshop on Energy Harvesting & Energy-Neutral Sensing Systems (ENSSys '19)*. Association for Computing Machinery, New York, NY, USA, 15–21. <https://doi.org/10.1145/3362053.3363489>
- [44] Stefan Schmid, Giorgio Corbellini, Stefan Mangold, and Thomas R. Gross. 2013. LED-to-LED visible light communication networks. In *Proceedings of the fourteenth ACM international symposium on Mobile ad hoc networking and computing*. ACM, Bangalore India, 1–10. <https://doi.org/10.1145/2491288.2491293>
- [45] Stefan Schmid, Thomas Richner, Stefan Mangold, and Thomas R. Gross. 2016. EnLighting: An Indoor Visible Light Communication System Based on Networked Light Bulbs. In *2016 13th Annual IEEE International Conference on Sensing, Communication, and Networking (SECON)*. IEEE, Unknown, 1–9. <https://doi.org/10.1109/SAHCN.2016.7732989>
- [46] Waseem Shariff, Mehdi Sefidgar Dilmaghani, Paul Kielty, Joe Lemley, Muhammad Ali Farooq, Faisal Khan, and Peter Corcoran. 2023. Neuromorphic Driver Monitoring Systems: A Computationally Efficient Proof-of-Concept for Driver Distraction Detection. *IEEE Open Journal of Vehicular Technology* 4 (2023), 836–848. <https://doi.org/10.1109/OJVT.2023.3325656>

- [47] Andrew Spielberg, Alanson Sample, Scott E. Hudson, Jennifer Mankoff, and James McCann. 2016. RapID: A Framework for Fabricating Low-Latency Interactive Objects with RFID Tags. In *Proceedings of the 2016 CHI Conference on Human Factors in Computing Systems (CHI '16)*. Association for Computing Machinery, New York, NY, USA, 5897–5908. <https://doi.org/10.1145/2858036.2858243>
- [48] Vamsi Talla, Michael Buettner, David Wetherall, and Joshua R Smith. 2013. Hybrid analog-digital backscatter platform for high data rate, battery-free sensing. In *2013 IEEE Topical Conference on Wireless Sensors and Sensor Networks (WiSNet)*. IEEE, IEEE, Unknown, 1–3.
- [49] Vamsi Talla, Mehrdad Hessar, Bryce Kellogg, Ali Najafi, Joshua R. Smith, and Shyamnath Gollakota. 2017. LoRa Backscatter: Enabling The Vision of Ubiquitous Connectivity. *Proc. ACM Interact. Mob. Wearable Ubiquitous Technol.* 1, 3 (Sept. 2017), 1–24. <https://doi.org/10.1145/3130970>
- [50] Ambiq Editorial Team. 2020. Apollo4. <https://ambiq.com/apollo4/>
- [51] University of Washington. 2023. *Wireless Identification and Sensing Platform*. University of Washington. <https://github.com/wisp>
- [52] Ambuj Varshney, Carlos Pérez-Penichet, Christian Rohner, and Thimo Voigt. 2017. LoRea: A Backscatter Architecture that Achieves a Long Communication Range. In *SenSys '17: Proceedings of the 15th ACM Conference on Embedded Network Sensor Systems*. Association for Computing Machinery, New York, NY, USA, 1–2. <https://doi.org/10.1145/3131672.3136996>
- [53] Ge Wang, Lubing Han, Yuance Chang, Yuting Shi, Chen Qian, Cong Zhao, Han Ding, Wei Xi, Cui Zhao, and Jizhong Zhao. 2023. Cross-technology Communication between Visible Light and Battery-free RFIDs. *Proceedings of the ACM on Interactive, Mobile, Wearable and Ubiquitous Technologies* 7, 3 (Sept. 2023), 1–20. <https://doi.org/10.1145/3610883>
- [54] Ziwei Wang, Yonhon Ng, Jack Henderson, and Robert Mahony. 2022. Smart Visual Beacons with Asynchronous Optical Communications using Event Cameras. In *2022 IEEE/RSJ International Conference on Intelligent Robots and Systems (IROS)*. IEEE, IEEE, Kyoto International Conference Center, Kyoto, Japan, 3793–3799.
- [55] Yue Wu, Purui Wang, Kenuo Xu, Lilei Feng, and Chenren Xu. 2020. Turboboosting Visible Light Backscatter Communication. In *Proceedings of the Annual conference of the ACM Special Interest Group on Data Communication on the applications, technologies, architectures, and protocols for computer communication*. ACM, Virtual Event USA, 186–197. <https://doi.org/10.1145/3387514.3406229>
- [56] Kenuo Xu, Chen Gong, Bo Liang, Yue Wu, Boya Di, Lingyang Song, and Chenren Xu. 2022. Low-Latency Visible Light Backscatter Networking with RetroMUMIMO. In *Proceedings of the 20th ACM Conference on Embedded Networked Sensor Systems*. ACM, Boston Massachusetts, 448–461. <https://doi.org/10.1145/3560905.3568507>
- [57] Xieyang Xu, Yang Shen, Junrui Yang, Chenren Xu, Guobin Shen, Guojun Chen, and Yunzhe Ni. 2017. PassiveVLC: Enabling Practical Visible Light Backscatter Communication for Battery-free IoT Applications. In *Proceedings of the 23rd Annual International Conference on Mobile Computing and Networking*. ACM, Snowbird Utah USA, 180–192. <https://doi.org/10.1145/3117811.3117843>
- [58] Hongfei Xue, Qiming Cao, Yan Ju, Haochen Hu, Haoyu Wang, Aidong Zhang, and Lu Su. 2023. M4esh: mmWave-Based 3D Human Mesh Construction for Multiple Subjects. In *Proceedings of the 20th ACM Conference on Embedded Networked Sensor Systems (SenSys '22)*. Association for Computing Machinery, New York, NY, USA, 391–406. <https://doi.org/10.1145/3560905.3568545>
- [59] Xiaoying Yang, Jacob Sayono, Jess Xu, Jiahao Nick Li, Josiah Hester, and Yang Zhang. 2022. MiniKers: Interaction-Powered Smart Environment Automation. *Proceedings of the ACM on Interactive, Mobile, Wearable and Ubiquitous Technologies* 6, 3 (Sept. 2022), 149:1–149:22. <https://doi.org/10.1145/3550287>
- [60] PENGYU ZHANG, Mohammad Rostami, Pan Hu, and Deepak Ganesan. 2016. Enabling Practical Backscatter Communication for On-body Sensors. In *Proceedings of the 2016 ACM SIGCOMM Conference (SIGCOMM '16)*. Association for Computing Machinery, New York, NY, USA, 370–383. <https://doi.org/10.1145/2934872.2934901>
- [61] Pengyu Zhang, Mohammad Rostami, Pan Hu, and Deepak Ganesan. 2016. Enabling practical backscatter communication for on-body sensors. In *Proceedings of the 2016 ACM SIGCOMM Conference*. ACM, New York, NY, USA, 370–383.
- [62] Xiaotong Zhang, Zhenjiang Li, and Jin Zhang. 2023. Synthesized Millimeter-Waves for Human Motion Sensing. In *Proceedings of the 20th ACM Conference on Embedded Networked Sensor Systems (SenSys '22)*. Association for Computing Machinery, New York, NY, USA, 377–390. <https://doi.org/10.1145/3560905.3568542>
- [63] Yang Zhang, Yasha Iravantchi, Haojian Jin, Swaran Kumar, and Chris Harrison. 2019. Sozu: Self-Powered Radio Tags for Building-Scale Activity Sensing. In *Proceedings of the 32nd Annual ACM Symposium on User Interface Software and Technology*. ACM, New Orleans LA USA, 973–985. <https://doi.org/10.1145/3332165.3347952>
- [64] Yi Zhou, Guillermo Gallego, and Shaojie Shen. 2021. Event-Based Stereo Visual Odometry. *IEEE Trans. Rob.* 37, 5 (March 2021), 1433–1450. <https://doi.org/10.1109/TRO.2021.3062252>